Measures and Linear Matrix Inequalities for Verification and Validation of a Flexible Aircraft with Adaptive Control

Daniel Wagner, Didier Henrion, Martin Hromčík

Measures and Linear Matrix Inequalities for Verification and Validation of a Flexible Aircraft with Adaptive Control

Daniel Wagner*, and Didier Henrion*†, and Martin Hromčík*

September 15, 2020

Abstract

Occupations measures and linear matrix inequality (LMI) relaxations (called the moment sums-of-squares or Lasserre hierarchy) can be used for verification and validation (VV) of adaptive control with piecewise polynomial dynamics and uncertain parameters. Specifically, we investigate the susceptibility to closed-loop instability for model reference adaptive control in the presence of large parameter uncertainties and/or unmodeled dynamics. In this document, we use our VV framework to validate a linear/polynomial F-16 model with MRAC and flexible dynamics with uncertain coupling. This is accomplished by addressing the uncertainties explicitly in the space of occupation measures and through exploiting sparsity for ordinary differential equations (ODEs). We show numerically that the closed-loop with simple model reference adaptive control (MRAC) can tolerate these phenomena at certain limits. This is achieved without the expense of conservative Lyapunov estimates and/or complex control law modifications. These numerical certificates guarantee finite-time convergence and the boundedness of all trajectories constrained in compact semi-algebraic sets. For comparison, worst-case behavior of the closed-loop is also obtained using Monte-Carlo simulations.

*D. Wagner, D. Henrion, and M. Hromčík are with the Faculty of Electrical Engineering, Czech Technical University in Prague, Technická 2, CZ-16626 Prague, Czech Republic {wagneda1, henridid, hromcik@fel.cvut.cz}

†D. Henrion is with CNRS, LAAS, 7 avenue du colonel Roche, F-31400 Toulouse, France henrion@laas.fr

1 Introduction

It is well established that model reference adaptive control (MRAC) is susceptible to closed-loop instability in the presence of system uncertainties and unmodeled dynamics [1]. To address this phenomenon, the authors of [2, 3, 4, 5, 6] proposed the use of "intelligent adaptive control". See also [7, 8, 9] where the authors propose an MRAC which can maintain closed-loop stability in the presence of uncertain parameters and unmodeled dynamics with respect to a set of initial conditions or under the assumption of persistency of excitation. Recently, the authors of [10, 11, 12, 13, 14] utilized an MRAC modification that permitted closed-loop stability in the presence of large uncertainties.

Using moment sum-of-squares (SOS) hierarchies with off-the-shelf-software technique is a state-of-the-art for verification and validation (VV) in aerospace. In particular, this approach is advantageous over Monte-Carlo when there are large uncertainties in the state space or when traditional VV methods are impermissible [15]. The authors of [16, 17] focus on polynomial dynamical models and polynomial SOS Lyapunov candidate functions. This methodology has also been applied to robust control law validation for SAFE-V [18] and validation of model reference adaptive control (MRAC) [19].

The procedure is similar to the results in [19]. First, our validation problem is written as a nonconvex nonlinear optimization problem over admissible trajectories. This problem is then written as its equivalent in the space of infinite dimensional measures. The problem is then relaxed by manipulating the measures via a problem of finite moment linear matrix inequality (LMI) relaxations. The solutions to our VV problem are primal in the sense that we optimize directly over the system trajectories. The well-established Lyapunov certificates can also be retrieved from the dual SOS LP problem. Off-the-shelf-software such as [20] and SDP solvers such as [21] or [22] can be used with our framework.

1.1 Main Contribution

Since MRAC cannot tolerate the presence large system uncertainties, they cannot be safely neglected in the design phase. For example, the coupling between the static and flexible modes in an aircraft is very difficult to model precisely and can lead to instability with MRAC. Model identification of the static and flexible modes is usually carried out separately through wind tunnel and vibration testing. The rest must be achieved by extensive simulation and flight testing.

To illustrate this problem, an F-16 model with unmodeled flexible dynamics and LQR + MRAC is considered. The closed-loop performance requirements can be expressed as a VV problem of polynomial dynamical optimization. These uncertain, bounded parameters in the unmodeled dynamics can be written explicitly in the space of occupation measures and do not require improved modeling accuracy. To reduce issues with scaling, exploiting parsimony for ODEs in introduced to partition the dynamics. Then the VV problem is solved with our framework.

The authors in [19] used polynomials to approximate the reference trajectory. This required partitioning the dynamics over several intervals in the time domain. For [23], using parsimony approximating the reference was introduced for the first time. As far as we know, this is the first time that a fully integrated VV framework is proposed for aircraft with flexible dynamics and MRAC.

Monte-Carlo simulations scale very poorly with the number of these uncertain parameters in the unmodeled system. If the state-space is not sufficiently explored for all uncertain parameters, there is good chance the simulations will not reveal unexplored, unsafe trajectories. This point is illustrated in a side-by-side comparison is made between the Monte-Carlo simulations and our framework for the F-16.

In the numerical examples, the ability for the LQR + MRAC to maintain acceptable command following in the presence of uncertain, unmodeled flexible dynamics is reflected in a cost function. If the uncertain parameters in the flexible dynamics are sufficiently small, it follows that the upper bound of this cost function is sufficiently small. Conversely, a cost function with a large upper bound is indicative of large unmodeled dynamics and unsafe trajectories.

Unlike the results of [7, 8, 9], we do not rely on a set of initial conditions or persistency of excitation. Compared to [10, 11, 12, 13, 14], control modifications are not used to address the unmodeled dynamics. Instead, it is demonstrated numerically that the upper tolerances of simple MRAC configuration using our VV framework. This is achieved by exploiting parsimony for ODEs similar to our results in [23]. Any uncertain parameters or initial condition mismatch can be addressed explicitly with our framework.

The organization of this document is as follows: Section 2 illustrates our main contribution by using a simple example, section 3 considers a closed-loop linear F-16 model coupled with uncertain flexible dynamics and MRAC, section 4 considers the model from [19] coupled with uncertain flexible dynamics, and section 5 contains a small discussion of our conclusions and future work.

2 Illustrative Simple Example

The proceeding problem draws directly the theoretical contributions provided in [24]. See also [19] for a practical example. The procedure for validating our uncertain models is illustrated in the simple example below. Consider the closed-loop linear parameter varying (LPV) system in the form of

$$\begin{bmatrix} \dot{\mathbf{x}}(t) \\ \dot{\mathbf{z}}(t) \end{bmatrix} = \begin{bmatrix} 0 & -1+k & 0 & 0 & 0 \\ 1+k & -5 & 0 & 0 & 0 \\ 0 & 0.1 & -10 & 0.1 & 0 \\ 0 & 0 & 0.1 & -1 & -0.1 \\ 0 & 0 & 0 & 1 & -1 \end{bmatrix} \begin{bmatrix} \mathbf{x}(t) \\ \mathbf{z}(t) \end{bmatrix} = \mathbf{f}(t, \mathbf{x}(t), \mathbf{z}(t), k), \quad \begin{matrix} \mathbf{x}(0) = \mathbf{x}_0, \\ \mathbf{z}(0) = \mathbf{z}_0, \end{matrix} \tag{1}$$

where $\mathbf{x}(t) = \begin{bmatrix} x_1(t) \ x_2(t) \end{bmatrix} \in \mathbb{R}^2$, $\mathbf{z}(t) = \begin{bmatrix} z_1(t) \ z_2(t) \ z_3(t) \end{bmatrix} \in \mathbb{R}^3$, and parameter $k \in \begin{bmatrix} -k_{max} \ k_{max} \end{bmatrix}, k_{max} \in \mathbb{R}_+$ is uncertain. Now suppose that eq. (1) is a closed loop model of some dynamical system such that the state trajectory of $x_1(T)$ reaches a smaller subset in finite time. In other words, we want find the initial state maximizing the norm of the terminal state with the concave quadratic term $J = \inf_{x_1(T)} -x_1(T)^2$ and given terminal time $T = 10$. There are also the initial constraints

$$\begin{aligned} \mathbf{x}(0) &\in \begin{bmatrix} -0.1 \ 0.1 \end{bmatrix}^2 \triangleq X_0, \\ \mathbf{z}(0) &\in \begin{bmatrix} -0.1 \ 0.1 \end{bmatrix}^3 \triangleq Z_0, \end{aligned}$$

the trajectory constraints

$$\begin{aligned} \mathbf{x}(t) &\in \begin{bmatrix} -1 \ 1 \end{bmatrix}^2 \triangleq X, \\ \mathbf{z}(t) &\in \begin{bmatrix} -1 \ 1 \end{bmatrix}^3 \triangleq Z, \end{aligned}$$

and the terminal constraints

$$\begin{aligned} \mathbf{x}(T) &\in \begin{bmatrix} -1 \ 1 \end{bmatrix}^2 \triangleq X_T, \\ \mathbf{z}(T) &\in \begin{bmatrix} -1 \ 1 \end{bmatrix}^3 \triangleq Z_T. \end{aligned}$$

This overall problem description can be collectively written as the poly-

nomial dynamical optimization problem

$$
\begin{aligned}
J = \inf_{x_1(T)} \quad & -x_1(T)^2 \\
\text{s.t.} \quad & \begin{bmatrix} \dot{\mathbf{x}}(t) \\ \dot{\mathbf{z}}(t) \end{bmatrix} = \mathbf{f}(t, \mathbf{x}(t), \mathbf{z}(t), k), \\
& \mathbf{x}(0) \in X_0, \quad \mathbf{x}(t) \in X, \quad \mathbf{x}(T) \in X_T, \\
& \mathbf{z}(0) \in Z_0, \quad \mathbf{z}(t) \in Z, \quad \mathbf{z}(T) \in Z_T, \\
& t \in [\,0,\, T\,], \quad k \in [\,-k_{max}\ k_{max}\,].
\end{aligned}
\tag{2}
$$

and is equivalent to the problem in the infinite-dimensional space of measures

$$
\begin{aligned}
J_\infty = \inf \quad & -\int x_1(T)^2 d\mu_T \\
\text{s.t.} \quad & \frac{\partial \mu}{\partial t} + \mathrm{div}\mathbf{f}\mu(t, \mathbf{x}, \mathbf{z}, k) + \mu_T = \mu_0 \\
& \int \mu_0 = 1
\end{aligned}
\tag{3}
$$

for all measures supported on $[0, T] \times X \times Z$, $\{0\} \times X_0 \times Z_0$, and $\{T\} \times X_T \times Z_T$ respectively. As discussed in [20], eq. (3) can be solved using a hierarchy of LMI relaxations.

The main takeaway here is that an abstract problem of measures can be manipulated by its corresponding moments generated by a finite number of truncated sequences. To avoid large semi-definite constraints in the final problem, a normalizing matrix $D = \mathrm{diag}(a_1, \ldots, a_5)$, $a_1, \ldots, a_5 \in \mathbb{R}_+$ is employed such that all trajectories, including the time domain, are constrained on the interval $[\,-1\ 1\,]$.

The procedure for expressing the validation problem in Gloptipoly 3 is no different. The script in A can be used to solve the the polynomial dynamical optimization problem eq. (2) with our framework using [21] as our main SDP solver. The computed upper bounds without parsimony can be found in Table 1. As k_{max} is increased, it is expected that the upper bound J will grow with it. Since the computational difficulty scales exponentially with the size of the largest moment SDP block, this problem cannot be solved beyond the fourth relaxation order. This procedure is analogous to searching the worst case eigenvalues $\lambda_{\max} = \max(\mathrm{re}(\mathrm{eig}(A(k))))$, which can be found in Table 2. The resulting script that solves the validation problem in section 2, with some scaling strategies to improve numerical behavior, can be found in A.

Table 1: Gloptipoly 3 + MOSEK Upper Bounds for Section 2

	$k_{\max} = 0.1$		$k_{\max} = 0.5$		$k_{\max} = 5$	
Rel Ord	**Upper Bnd** J	**CPU [s]**	**Upper Bnd** J	**CPU [s]**	**Upper Bnd** J	**CPU [s]**
1	1.41×10^{-2}	2.18	1.71×10^{-2}	2.17	1	2.08
2	8.03×10^{-4}	5.13	1.44×10^{-3}	5.46	1	4.68
3	2.84×10^{-4}	1.22×10^{2}	8.39×10^{-4}	1.08×10^{2}	1	1.25×10^{2}
4	2.67×10^{-4}	2.13×10^{3}	8.30×10^{-4}	2.88×10^{3}	1	3.90×10^{3}
5	-	-	-	-	-	-

Table 2: Largest Eigenvalues for Section 2

$k_{\max}$	$\lambda_{\max}$
0.1	-2.07×10^{-1}
0.5	-1.55×10^{-1}
5	3

2.1 Exploiting Parsimony for ODEs

The results of section 2 will now be repeated by exploiting parsimony for ODEs. The main advantage to this approach is that it reduces the size of the largest SDP block. Consequently, our framework can be used to validate problems that are larger in size. First, eq. (1) can be rewritten as

$$\dot{\mathbf{x}}(t) = \mathbf{f_1}(t, \mathbf{x}(t), k), \quad y(t) = x_2(t) \tag{4}$$

$$\dot{\mathbf{z}}(t) = \mathbf{f_2}(t, \mathbf{z}(t), y(t)), \tag{5}$$

where dynamics $\mathbf{f_1}(\cdot) \in \mathbb{R}[\, t \ \mathbf{x}(t) \ k \,]$ are autonomous and $y(t) = x_2(t) \in \mathbb{R}$ can be interpreted as a control input to $\mathbf{f_2}(\cdot) \in \mathbb{R}[\, t \ \mathbf{z}(t) \ y(t) \,]$. Using the same polynomial dynamical optimization problem eq. (2) and partitioned dynamics eq. (5), the problem of measures can be written as

$$\begin{aligned} J_\infty = \ \inf \quad & -\int x_1(T)^2 d\mu_T \\ \text{s.t.} \quad & \frac{\partial \mu}{\partial t} + \text{div}\mathbf{f_1}\mu(t, \mathbf{x}, k) + \mu_T = \mu_0 \\ & \frac{\partial \nu}{\partial t} + \text{div}\mathbf{f_2}\nu(t, \mathbf{z}, y) + \nu_T = \nu_0 \\ & \pi_{t,\mathbf{y}\#}\mu = \pi_{t,\mathbf{y}\#}\nu \\ & \int \mu_0 = 1, \quad \int \nu_0 = 1, \end{aligned} \tag{6}$$

with marginal $\pi_{t,\mathbf{y}\#}\mu$, respectively $\pi_{t,\mathbf{y}\#}\nu$, of measure μ, respectively ν, with respect to variables t, $\mathbf{y}$. The moment LMI relaxation problem is modified

Table 3: Gloptipoly 3 + MOSEK Upper Bounds for Section 2.1

	$k_{\max} = 0.1$		$k_{\max} = 0.5$		$k_{\max} = 5$	
Rel Ord	**Upper Bnd** J	**CPU [s]**	**Upper Bnd** J	**CPU [s]**	**Upper Bnd** J	**CPU [s]**
1	1.41×10^{-2}	1.64	1.71×10^{-2}	5.32×10^{-1}	1	4.00×10^{-1}
2	8.03×10^{-4}	1.10	1.44×10^{-3}	9.17×10^{-1}	1	8.29×10^{-1}
3	2.87×10^{-4}	2.86	8.38×10^{-4}	2.61	1	2.49
4	2.67×10^{-4}	9.58	8.31×10^{-4}	1.01×10^{1}	1	8.64
5	2.67×10^{-4}	4.50×10^{1}	8.30×10^{-4}	4.88×10^{1}	1	5.04×10^{1}

accordingly. The results can be found in Table 3. As illustrated, similar upper bounds can be achieved. Since the size of the largest moment SDP block is reduced in this configuration, the problem size can be solved up to the fifth relaxation order. The overall maximum problem size is reduced by 2. This property will be exploited to solve problems with a large number of states in the proceeding sections.

The theoretical background for these results were first noted in [25]. In the proceeding section, this methodology for exploiting parsimony for ODEs is unchanged. If our problem can be written in the form similar to eq. (5) and eq. (6), then it is possible to proceed by solving our VV problem in Gloptipoly 3 using our framework.

3 Flexible Dynamics for a F-16 Linear Model

Our objective is to validate a linear F-16 short period aircraft model augmented with adaptive feedback, uncertain parameters, and flexible dynamics using our VV framework. The procedure for implementing our framework is rather straight forward. In section 3.1 we discuss the simplified uncertain aeroelastic model and its closed loop configuration. Although the rigid body and flexible modes are well-defined, their coupling is not. For the coupling uncertain, bounded parameters $k_1,\ k_2,\ k_3 \in [\, -k_{max}\ k_{max}\,]$, $k_{max} \in \mathbb{R}_+$ are used. After writing the problem in its compact form, control law validation problem is explicitly stated in section 3.2. The problem is then partitioned by exploiting parsimony for ODEs. The number of uncertain parameters are gradually increased. Finally, the model and its uncertainties are addressed explicitly using our framework and then validated under adverse flight conditions. In total, there are three cases:

1. k_1 is *uncertain*, k_2 and k_3 are *known*
2. k_1 and k_3 are *uncertain*, k_2 is *known*
3. k_1, k_2, and k_3 are *uncertain*

3.1 Closed-Loop Configuration

Consider the short-period dynamics of a linear F-16 aircraft coupled with flexible dynamics

$$\dot{\mathbf{x}}_{\mathbf{p}}(t) = \underbrace{\left[\begin{smallmatrix} -1.0189 & +0.9051 \\ +0.8223 & -1.0774 \end{smallmatrix}\right]}_{A_{\mathrm{p}}} \mathbf{x}_{\mathbf{p}}(t) + \underbrace{\left[\begin{smallmatrix} -0.0022 \\ -0.1756 \end{smallmatrix}\right]}_{B_{\mathrm{p}}} \underbrace{0.7}_{\Lambda} \big(u(t) + \delta(\mathbf{x}_{\mathbf{p}}(t))\big) \tag{7}$$

$$+ \underbrace{\left[\begin{smallmatrix} -0.0022k_1 & 0 \\ -0.1756k_1 & 0 \end{smallmatrix}\right]}_{B_{\mathrm{p}}H(k_1)^T} \mathbf{z}(t), \quad \mathbf{x}_{\mathbf{p}}(0) = \mathbf{x}_{\mathbf{p}_0} \tag{8}$$

$$\dot{\mathbf{z}}(t) = \underbrace{\left[\begin{smallmatrix} -0.5 & 6.3 \\ -6.3 & -0.5 \end{smallmatrix}\right]}_{F} \mathbf{z}(t) + \underbrace{\left[\begin{smallmatrix} k_3 \\ k_2 \end{smallmatrix}\right]}_{G(k_2,k_3)^T} \mathbf{x}_{\mathbf{p}}(t), \quad \mathbf{z}(0) = \mathbf{z}_0 \tag{9}$$

where $\mathbf{x}_{\mathbf{p}}(t) = \left[\begin{smallmatrix} \alpha(t) & q(t) \end{smallmatrix}\right] \in \mathbb{R}^2$ are the short period dynamics, $\alpha(t)$ is the angle of attack, $q(t)$ is the pitch-rate, $\mathbf{z}(t) = \left[\begin{smallmatrix} z_1(t) & z_2(t) \end{smallmatrix}\right] \in \mathbb{R}^2$ are states related to the modal form of a considered dominant aeroelastic mode. Matrix F represents a 5.2 Hz first bending mode of the aircraft [26]. There is also measurable control input $u(t) \in \mathbb{R}$, control effectiveness $\Lambda \in \mathbb{R}_+$, the in state uncertainty

$$\delta(\mathbf{x}_{\mathbf{p}}(t)) = \underbrace{\left[\begin{smallmatrix} -0.0468 & -0.0982 \end{smallmatrix}\right]}_{K_{pert}} \mathbf{x}_{\mathbf{p}}(t), \tag{10}$$

and uncertain parameters representing the coupling of the rigid body and flexible dynamics $k_1, k_2, k_3 \in \left[\begin{smallmatrix} -k_{max} & k_{max} \end{smallmatrix}\right]$.

Our control objective is design a control law $u(t)$ to reject the in state disturbance eq. (10) and asymptotically track the reference trajectory $\mathbf{x}_{\mathbf{r}}(t) = \left[\begin{smallmatrix} \alpha_{\mathrm{r}}(t) & q_{\mathrm{r}}(t) \end{smallmatrix}\right]$ generated by the dynamics

$$\dot{\mathbf{x}}_{\mathbf{r}}(t) = A_{\mathrm{r}}\mathbf{x}_{\mathbf{r}}(t) + B_{\mathrm{r}}c(t) \tag{11}$$

where $c(t) \in \mathbb{R}$ is a bounded command signal. The *desired closed loop* dynamics are derived using the nominal feedback control law [27]

$$u_{\mathrm{n}}(t) = \underbrace{\left[\begin{smallmatrix} -4.7432 & 2.3163 \end{smallmatrix}\right]}_{K_1} \mathbf{x}_{\mathbf{p}}(t) - \underbrace{4.3396}_{K_2} c(t), \tag{12}$$

such that $A_{\mathrm{r}} = A_{\mathrm{p}} - B_1$ is Hurwitz and $B_{\mathrm{r}} = B_{\mathrm{p}}K_2$. To reject exogenous disturbance and improve tracking performance an the adaptive feedback control law

$$u_{\mathrm{a}}(t) = -\hat{\mathbf{W}}(t)^T \Phi(\mathbf{x}_{\mathbf{p}}(t)) \tag{13}$$

is also included with basis function $\Phi_i(\mathbf{x_p}(t)) = (1+e^{\mathbf{x_p}i})^{-1}$ and $\hat{\mathbf{W}}(t) \in \mathbb{R}^2$ satisfies the weight update law

$$\dot{\hat{\mathbf{W}}}(t) = \underbrace{[\,^{\epsilon}{}_{100}\,]}_{\Gamma}\big(\Phi\big(\mathbf{x_p}(t)\big)\mathbf{e}^T(t)PB_{\mathrm{p}} + \underbrace{5(\mathbf{e}^T(t)PB_{\mathrm{p}})^2\hat{\mathbf{W}}(t)}_{\dot{\hat{\mathbf{W}}}_m(t)}\big), \quad \hat{\mathbf{W}}(0) = \hat{\mathbf{W}}_0 \tag{14}$$

where $\epsilon << 1$, error dynamics $\mathbf{e}(t) = \mathbf{x_p}(t) - \mathbf{x_r}(t)$, $\dot{\hat{\mathbf{W}}}_m(t)$ is the error modification [28], and positive definite symmetric $P \in \mathbb{R}^{2\times 2}$ is the unique solution to the Lyapunov equation

$$0 = A_{\mathrm{r}}^T P + PA_{\mathrm{r}} + 10I_{2\times 2}. \tag{15}$$

The *combined* nominal/adaptive feedback control law can be written as

$$u(t) = u_{\mathrm{n}}(t) + u_{\mathrm{a}}(t) \tag{16}$$

which was used in eq. (8). In practice, Lyapunov analysis only informs us about the ultimate stability of the closed-loop system if the unmodeled dynamics are neglected. There at least exists a Lyapunov candidate function such that the longitudinal dynamics eq. (8) subject to the control and weight update law eqs. (14) and (16) has the property $\lim_{t\to\infty} e(t) = 0$. Consequently, learning rates of eq. (14) were tuned to reject disturbances and achieve tracking without the flexible dynamics.

It's of practical interest to know if the MRAC can tolerate unmodeled dynamics and uncertain parameters of a certain magnitude. In proceeding section it is shown numerically when the unmodeled dynamics with uncertain parameters can be neglected without using control modifications. These achieved upper bounds are significantly less conservative than norm approximations found in the Lyapunov analysis.

To set up the problem for our VV framework, the compact form of the closed-loop model can now be written by combining eq. (8), eq. (9), eq. (11),eq. (14), and eq. (16) to get

$$\begin{aligned}
&\dot{\mathbf{x}}_{\mathbf{1}}(t) = \mathbf{f_1}(t, \mathbf{x_1}(t), c(t)), && y_1(t) = \alpha_{\mathrm{r}}(t), && \mathbf{x_1}(0) = \mathbf{x_{10}}\\
&\dot{\mathbf{x}}_{\mathbf{2}}(t) = \mathbf{f_2}(t, \mathbf{x_2}(t), y_1(t), y_3(t), k_1), && \mathbf{y_2}(t) = \mathbf{x_p}(t), && \mathbf{x_2}(0) = \mathbf{x_{20}}\\
&\dot{\mathbf{x}}_{\mathbf{3}}(t) = \mathbf{f_3}(t, \mathbf{x_3}(t), \mathbf{y_2}(t), k_2, k_3), && y_3(t) = z_1(t), && \mathbf{x_3}(0) = \mathbf{x_{30}}
\end{aligned} \tag{17}$$

where $\mathbf{x_1}(t) = \mathbf{x_r}(t) \in \mathbb{R}^2$, $\mathbf{x_2}(t) = [\,\mathbf{x_p}(t),\, \hat{\mathbf{W}}(t)\,] \in \mathbb{R}^3$, $\mathbf{x_3}(t) = \mathbf{z}(t) \in \mathbb{R}^2$, and $\mathbf{y_2}(t) \in \mathbb{R}^2$.

3.2 Validation Problem & Main Results

We want to validate our closed-loop model in its compact form eq. (17) by finding the initial state that maximizes the norm of the concave cost function of the error dynamics $J = -\left\|\mathbf{e}(T)\right\|_2^2$ with given command signal $c(t) = 0.1$ and terminal time $T = 20$. If it can be shown that for every chosen initial state

$$\begin{aligned}
&\mathbf{x_1}(0) \in \left[\,-0.2\ 0.2\,\right]^2 \triangleq X_{10}\\
&\mathbf{x_2}(0) \in \left[\,-0.2\ 0.2\,\right]^2 \times \left[\,-1\times 10^{-6},\ 1\times 10^{-6}\,\right] \triangleq X_{20}\\
&\mathbf{x_3}(0) \in \left[\,-0.2\ 0.2\,\right]^2 \triangleq X_{30}
\end{aligned}$$

all trajectories remain bounded in the box

$$\begin{aligned}
&\mathbf{x_1}(t) \in \left[\,-1\ 1\,\right]^2 \triangleq X_1\\
&\mathbf{x_2}(t) \in \left[\,-1\ 1\,\right]^2 \times \left[\,-5,\ 5\,\right] \triangleq X_2\\
&\mathbf{x_3}(t) \in \left[\,-1\ 1\,\right]^2 \triangleq X_3
\end{aligned}$$

until they reach the final state belonging to the set $\mathbf{e}(T) \in \{J \leq 3\times 10^{-3}\} \triangleq X_{1T}$, then the control law is validated. The overall description can be expressed by its polynomial dynamical optimization problem

$$\begin{aligned}
J = \inf_{x}\quad & -\left\|\mathbf{e}(T)\right\|_2^2\\
\text{s.t.}\quad & \dot{\mathbf{x}}_1(t) = \mathbf{f_1}(t, \mathbf{x_1}(t), c(t))\\
& \dot{\mathbf{x}}_2(t) = \mathbf{f_2}(t, \mathbf{x_2}(t), y_1(t), y_3(t), k_1)\\
& \dot{\mathbf{x}}_3(t) = \mathbf{f_3}(t, \mathbf{x_3}(t), \mathbf{y_2}(t), k_2, k_3)\\
& \mathbf{x_1}(0) \in X_{10},\quad \mathbf{x_1}(t) \in X_1,\quad \mathbf{x_1}(T) \in X_{1T},\\
& \mathbf{x_2}(0) \in X_{20},\quad \mathbf{x_2}(t) \in X_2,\quad \mathbf{x_2}(T) \in X_2,\\
& \mathbf{x_3}(0) \in X_{30},\quad \mathbf{x_3}(t) \in X_3,\quad \mathbf{x_3}(T) \in X_3,\\
& t \in \left[\,0,\ T\,\right],\quad u \in \left[\,-k_{max}\ k_{max}\,\right].
\end{aligned} \tag{18}$$

Its approximation in the space of infinite dimensional measures using parsimony can be written as

$$
\begin{aligned}
J_\infty = \inf \quad & -\int \|\mathbf{e}(T)\|_2^2 \, d\mu_T \\
\text{s.t.} \quad & \frac{\partial \mu}{\partial t} + \text{div}\mathbf{f_1}\mu(t, \mathbf{x_1}) + \mu_T = \mu_0 \\
& \frac{\partial \nu}{\partial t} + \text{div}\mathbf{f_2}\nu(t, \mathbf{x_2}, y_1, y_3, k_1) + \nu_T = \nu_0 \\
& \frac{\partial \xi}{\partial t} + \text{div}\mathbf{f_3}\xi(t, \mathbf{x_3}, \mathbf{y_2}, k_2, k_3) + \xi_T = \xi_0 \\
& \pi_{t,y_1,\#}\mu = \pi_{t,y_1,\#}\nu \\
& \pi_{t,\mathbf{y_2},y_3,\#}\mu = \pi_{t,\mathbf{y_2},y_3,\#}\xi \\
& \int \mu_0 = 1, \quad \int \nu_0 = 1, \quad \int \xi_0 = 1
\end{aligned}
\tag{19}
$$

and its respective moment LMI relaxations problem is modified accordingly. The same marginals of their respective measures from section 3 are also used. In total the overall size of the problem is reduced by 5 variables using parsimony. and its respective moment LMI relaxations problem is modified accordingly. The marginal $\pi_{t,y_1,\#}\mu$, respectively $\pi_{t,y_1,\#}\nu$, on measure μ, respectively ν, are with respect to variables t, y_1. There is also marginal $\pi_{t,\mathbf{y_2},y_3,\#}\mu$, respectively $\pi_{t,\mathbf{y_2},y_3,\#}\xi$, on measure μ, respectively ξ, with respect to variables t, $\mathbf{y_2}$, andy_3. Similar to [23], partitioning the dynamics and approximating the reference trajectory [23] allows using a command signal without using piecewise approximations [19]. In total the problem is reduced by 4 variables using parsimony.

The main results can be found below. In Table 4 an uncertain $k_1 \in [\,-k_{max}\ k_{max}\,]$ is considered with fixed $k_2 = -0.1,\ k_3 = 0.1$. Similar upper bounds were achieved for all values of k_{max}, which indicates tolerance from the MRAC in the presence of unmodeled flexible dynamics. Likewise, in Table 5 let $k_1,\ k_3 \in [\,-k_{max}\ k_{max}\,]$ and fix $k_2 = -0.1$. Lastly, in Table 6 there is also $k_1,\ k_3,\ k_2 \in [\,-k_{max}\ k_{max}\,]$. The upper bounds achieved are larger than those obtained for the one uncertain parameter case. At $k_{max} = 10$, the upper bound violates the terminal constraint which indicates the presence of unstable trajectories for two or three uncertain parameters.

The simulation results using Monte-Carlo can be found in Table 7 and Figures 1 to 9. These simulations were obtained using evenly spaced initial conditions and Newton's Method. Red lines in the plot represent the desired closed loop performance. The maximum costs were obtained by finding the

Table 4: Gloptipoly 3 + MOSEK LQR + MRAC Upper Bounds for Section 3 - Uncertain k_1 ($k_2,\ k_3 = -0.1$)

	$k_{\max} = 0.1$		$k_{\max} = 1$		$k_{\max} = 10$	
Rel Ord	**Upper Bnd** J	**CPU [s]**	**Upper Bnd** J	**CPU [s]**	**Upper Bnd** J	**CPU [s]**
1	1.96×10^{-1}	2.24	2.04×10^{-1}	7.34×10^{-1}	3.19×10^{-1}	6.13×10^{-1}
2	8.14×10^{-4}	4.80	9.46×10^{-4}	5.03	7.29×10^{-3}	4.15
3	2.01×10^{-4}	1.14×10^{2}	1.76×10^{-4}	1.18×10^{2}	7.04×10^{-4}	1.09×10^{2}

Table 5: Gloptipoly 3 + MOSEK LQR + MRAC Upper Bounds for Section 3 - Uncertain $k_1,\ k_3$ ($k_2 = -0.1$)

	$k_{\max} = 0.1$		$k_{\max} = 1$		$k_{\max} = 10$	
Rel Ord	**Upper Bnd** J	**CPU [s]**	**Upper Bnd** J	**CPU [s]**	**Upper Bnd** J	**CPU [s]**
1	3.19×10^{-1}	1.90	2.08×10^{-1}	1.40	1.24	6.83×10^{-1}
2	7.29×10^{-3}	7.54	1.09×10^{-3}	7.73	1.24	5.57
3	7.04×10^{-4}	1.62×10^{2}	1.09×10^{-3}	1.41×10^{2}	1.24	1.25×10^{2}

worst case trajectories in the simulation. In Figures 6 and 9 and Table 7, the system becomes unstable for $k_{max} = 10$. This reflects our results obtained in Table 6. As shown in Table 7, increasing the number of uncertainties becomes costly. Conversely, you also risk missing unsafe trajectories if your parameter spacing is too sparse. In juxtaposition, similar upper bounds can be achieved using our framework with equivalent or less computation time.

4 Flexible Dynamics for an F-16 Polynomial Model

A nonlinear polynomial short period F-16 aircraft model augmented with adaptive feedback and in the presence of flexible dynamics is now considered. The model itself and its feedback were used previously in [19]. The same flexible dynamics from eq. (9) and the uncertain parameters $k_1,\ k_2,\ k_3 \in [-k_{max}\ k_{max}]$, $k_{max} \in \mathbb{R}_+$ are used. The procedure remains similar. After

Table 6: Gloptipoly 3 + MOSEK LQR + MRAC Upper Bounds for Section 3 - Uncertain $k_1,\ k_3,\ k_2$

	$k_{\max} = 0.1$		$k_{\max} = 1$		$k_{\max} = 10$	
Rel Ord	**Upper Bnd** J	**CPU [s]**	**Upper Bnd** J	**CPU [s]**	**Upper Bnd** J	**CPU [s]**
1	1.96×10^{-1}	1.75	2.14×10^{-1}	9.82×10^{-1}	1.24	8.14×10^{-1}
2	7.49×10^{-4}	8.72	1.93×10^{-3}	9.17	1.24	8.89
3	1.03×10^{-4}	2.55×10^{2}	3.10×10^{-4}	2.18×10^{2}	1.24	2.97×10^{2}

Table 7: Monte-Carlo Upper Bounds for Section 3

	Uncertain κ		**Uncertain κ, ζ**		**Uncertain κ, η, ζ**	
$k_{\max}$	**Upper Bnd J**	**CPU [s]**	**Upper Bnd J**	**CPU [s]**	**Upper Bnd J**	**CPU [s]**
0.1	3.75×10^{-8}	4.09×10^{1}	3.75×10^{-8}	1.76×10^{2}	3.75×10^{-8}	8.81×10^{2}
1	4.00×10^{-8}	4.08×10^{1}	4.36×10^{-8}	4.99×10^{2}	5.40×10^{-8}	9.21×10^{2}
10	7.70×10^{-8}	4.06×10^{1}	6.82×10^{-1}	2.58×10^{2}	1.13	8.77×10^{2}

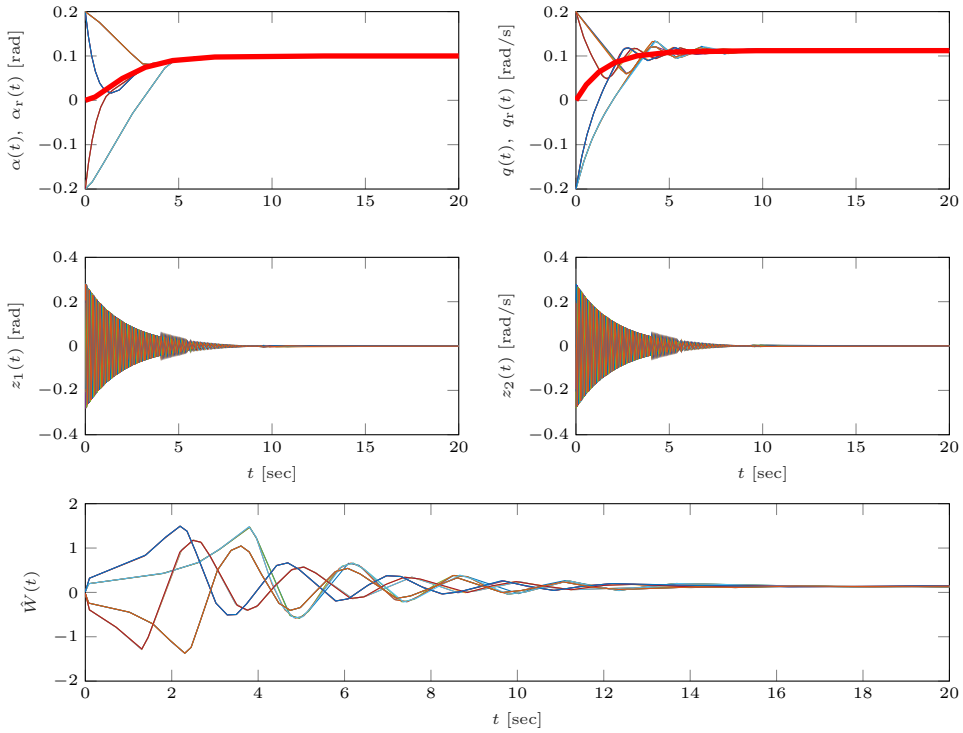

Figure 1: Monte-Carlo Worst Case for Section 3 - Uncertain k_1 - ($k_1 = 0.1$, $k_2 = -0.1$, $k_3 = -0.1$)

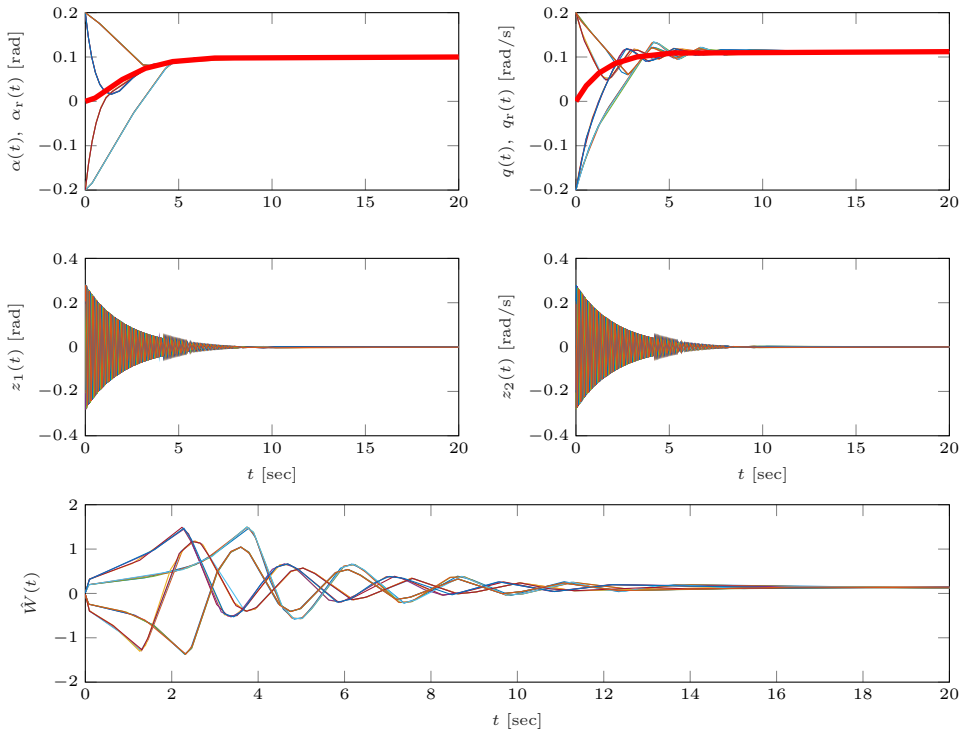

Figure 2: Monte-Carlo Worst Case for Section 3 - Uncertain k_1 - ($k_1 = 1$, $k_2 = -0.1$, $k_3 = -0.1$)

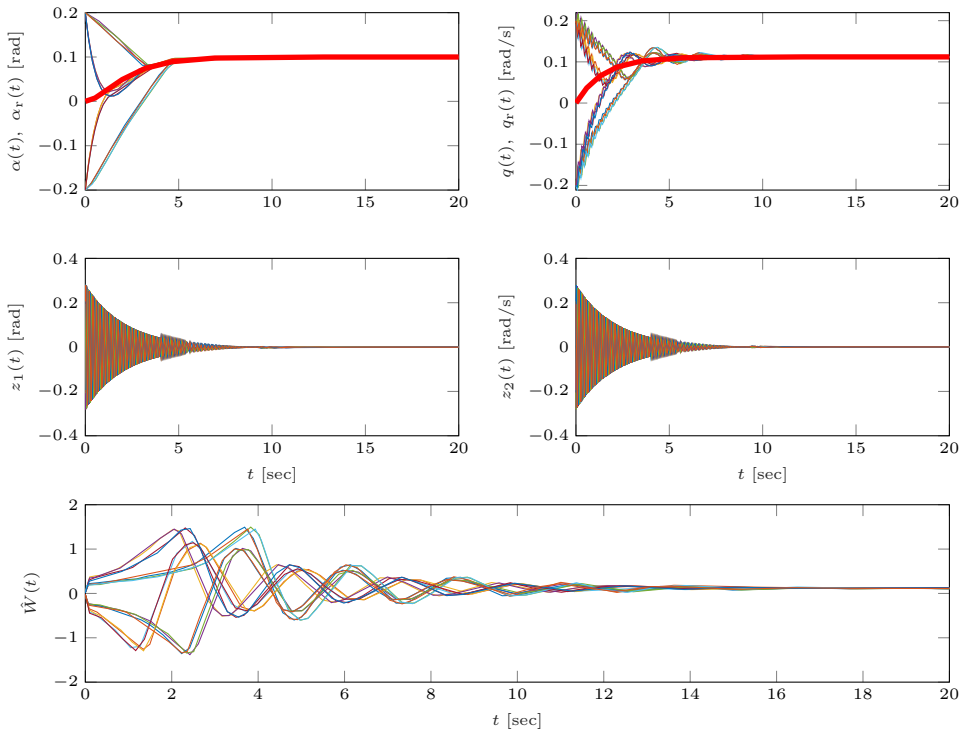

Figure 3: Monte-Carlo Worst Case for Section 3 - Uncertain k_1 - ($k_1 = 10$, $k_2 = -0.1$, $k_3 = -0.1$)

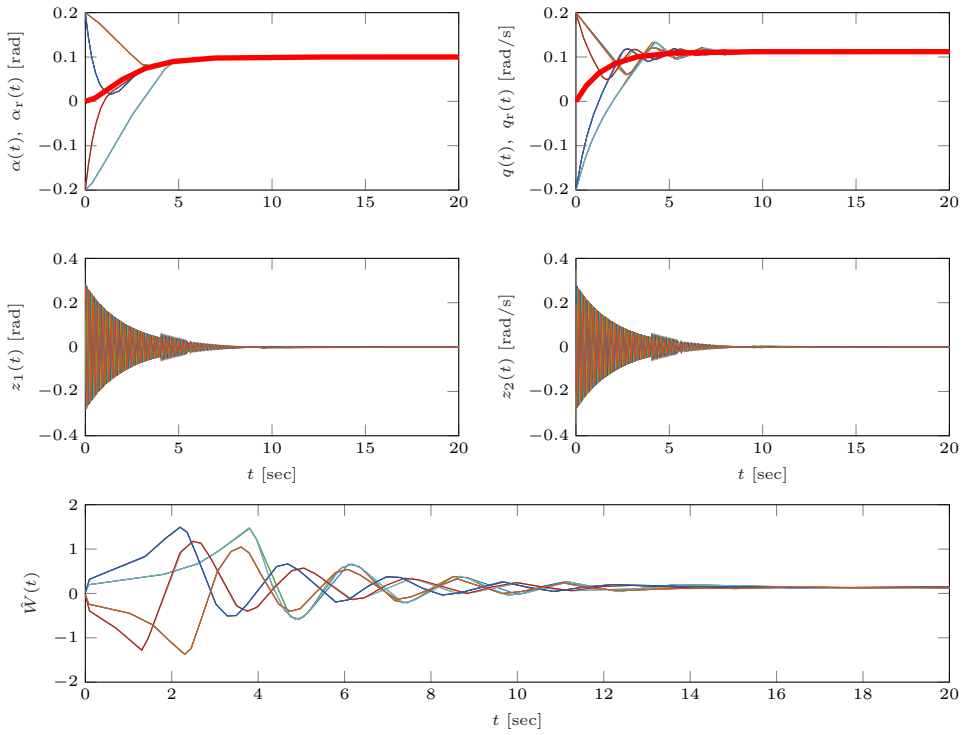

Figure 4: Monte-Carlo Worst Case for Section 3 - Uncertain $k_1,\ k_3$ - ($k_1 = 0.1$, $k_2 = -0.1$, $k_3 = 0.1$)

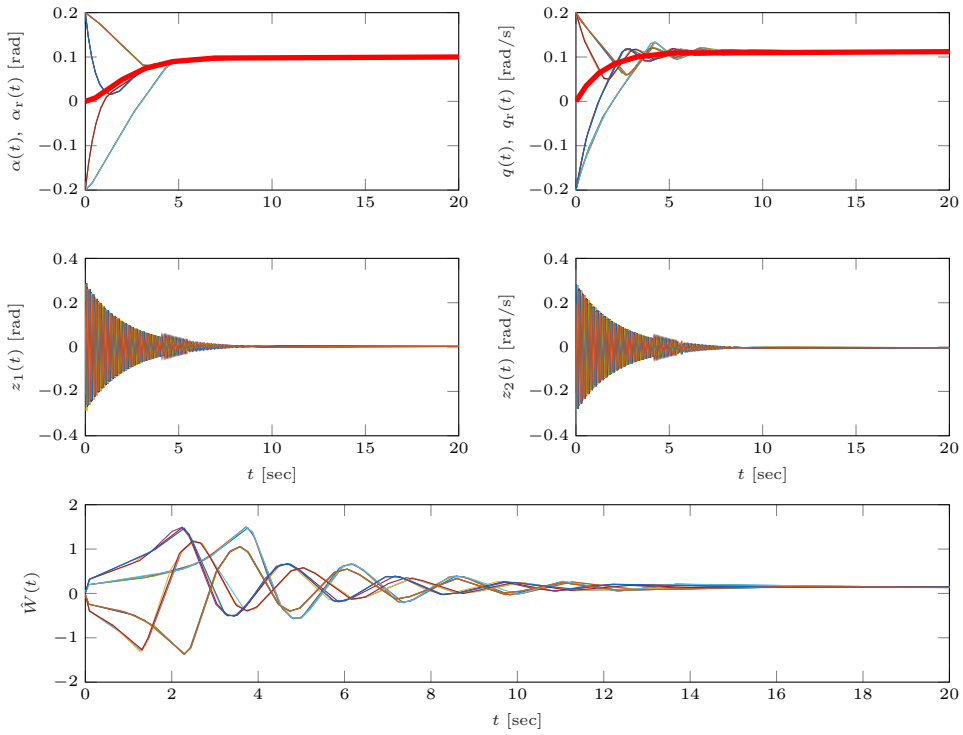

Figure 5: Monte-Carlo Worst Case for Section 3 - Uncertain $k_1,\ k_3$ - ($k_1 = 1,\ k_2 = -0.1,\ k_3 = -1$)

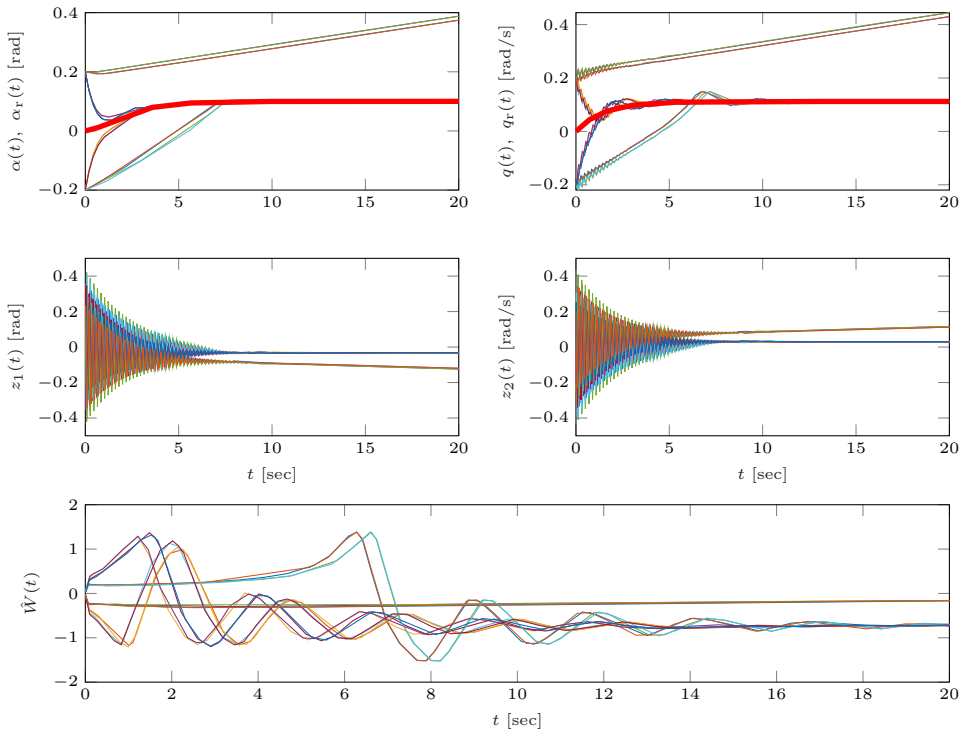

Figure 6: Monte-Carlo Worst Case for Section 3 - Uncertain $k_1,\ k_3$ - ($k_1 = 10,\ k_2 = -0.1,\ k_3 = -10$)

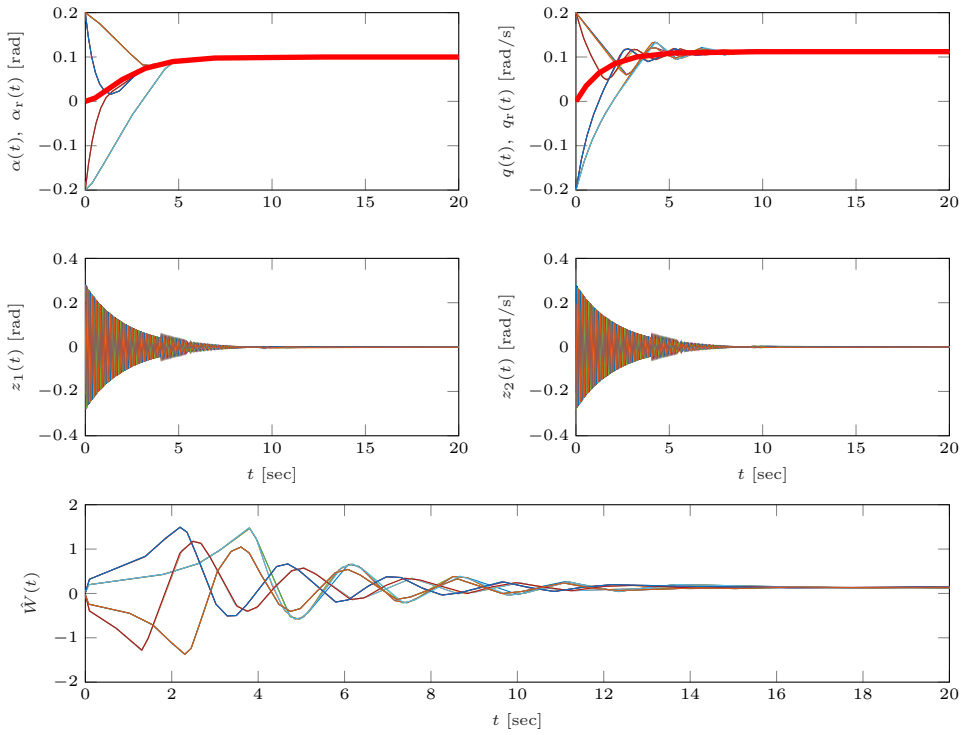

Figure 7: Monte-Carlo Worst Case for Section 3 - Uncertain $k_1,\ k_2,\ k_3$ - $(k_1 = 0.1,\ k_2 = -0.1,\ k_3 = -0.1)$

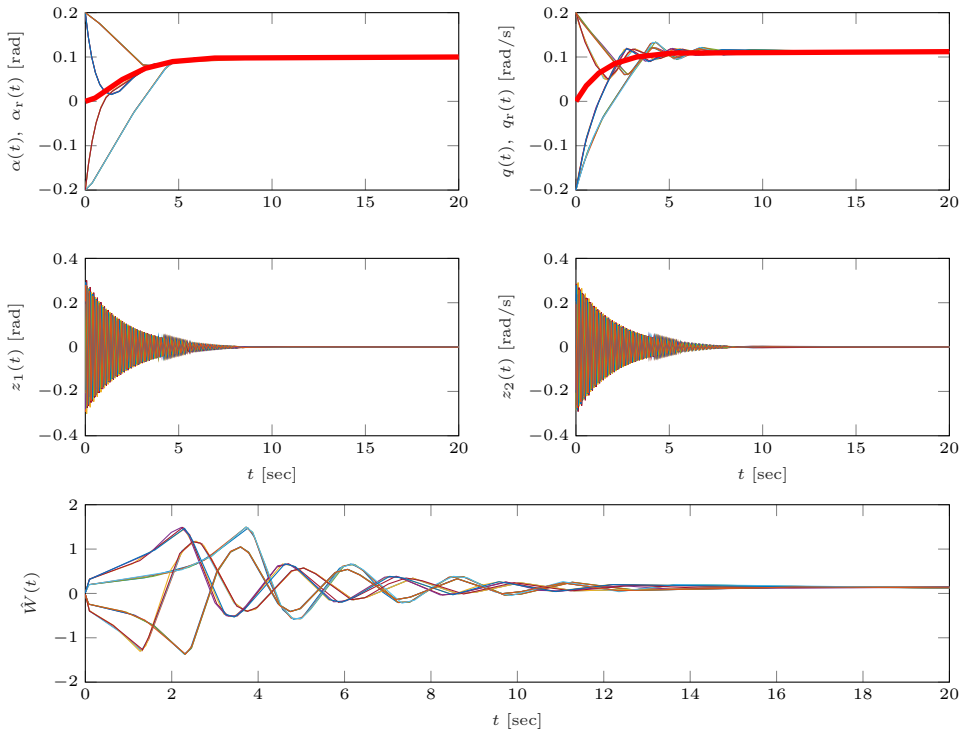

Figure 8: Monte-Carlo Worst Case for Section 3 - Uncertain $k_1,\ k_2,\ k_3$ - $(k_1 = 1,\ k_2 = -1,\ k_3 = -1)$

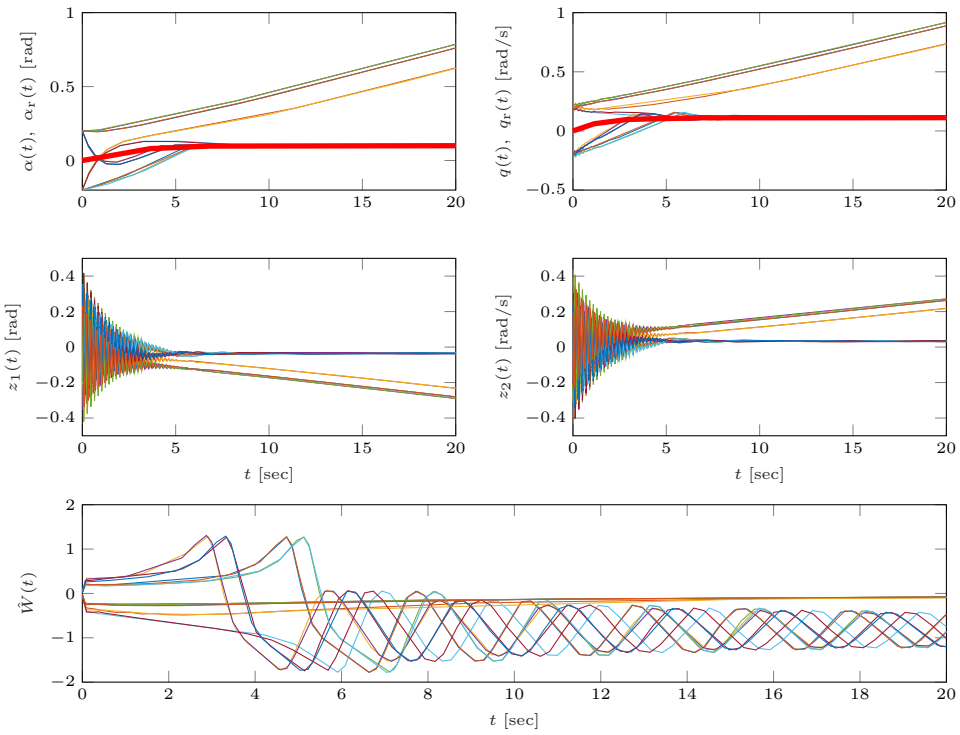

Figure 9: Monte-Carlo Worst Case for Section 3 - Uncertain $k_1,\ k_2,\ k_3$ - $(k_1 = 10,\ k_2 = -10,\ k_3 = -10)$

problem is presented in its compact form, it is written as a polynomial dynamical optimization problem, and then as its approximated partitioned form in the space of infinite measures using parsimony. Lastly, the model and its uncertainties are addressed explicitly using our framework and then validated under adverse flight conditions. In total, there are two cases:

1. k_1 is *uncertain*, k_2 and k_3 are *known*
2. k_1 and k_3 are *uncertain*, k_2 is *known*

4.1 Closed-Loop Configuration

Now consider a polynomial F-16 model with flexible dynamics

$$\dot{e}_\alpha(t) = \alpha(t) - c(t) \tag{20}$$

$$\dot{\mathbf{x}}_\mathbf{p}(t) = \mathbf{f}_\mathbf{p}(t, \mathbf{x}_\mathbf{p}(t), \Lambda u(t)) + B_\mathrm{p} H(k_1)^T \mathbf{z}(t) \tag{21}$$

$$\dot{\mathbf{z}}(t) = F\mathbf{z}(t) + G(k_2, k_3)^T \mathbf{x}_\mathbf{p}(t) \tag{22}$$

where $\mathbf{x}_\mathbf{p}(t) = \left[\, \alpha(t),\, q(t) \,\right]$ and polynomial $\mathbf{f}_\mathbf{p}(t, \mathbf{x}(t), \Lambda u(t)) \in \mathbb{R}^2\left[\, t,\, \mathbf{x_p} \,\right]$ are taken from [19]. The same matrices from section 3.1 B_p, F, $H(k_1)$, and $G(k_2, k_3)$ were used. The same uncertain parameter $k_1,\ k_2,\ k_3 \in \left[\, -k_{max}\ k_{max} \,\right]$ and reduced control effectiveness $\Lambda = 0.7$ were also used.

Our control objective is similar. We want to asymptotically track the reference dynamics eq. (11) and command signal $c(t)$. With the *augmented* AOA tracking dynamics eq. (20), the new nominal control law becomes

$$u_\mathrm{n}(t) = -\underbrace{\left[\, -10.0000\ -10.8756\ -6.0565 \,\right]}_{K} \mathbf{x}_\mathbf{p}(t) \tag{23}$$

and was obtained using the LQR method [29]. Likewise, $A_\mathrm{r} = A_\mathrm{p} - B_\mathrm{p} K$ is Hurwitz, $B_\mathrm{p} = \left[\, 0\ B_\mathrm{p} \,\right]^T$ and $B_\mathrm{r} = \left[\, -1\ 0\ 0 \,\right]^T$ for eq. (11). A similar adaptive feedback law $u_\mathrm{a}(t) = \hat{\mathbf{W}}(t)^T \Phi(\mathbf{x}_\mathbf{p}(t))$ is also used

$$\dot{\hat{\mathbf{W}}}(t) = \underbrace{\begin{bmatrix} \epsilon & & \\ & \epsilon & \\ & & 100 \end{bmatrix}}_{\Gamma} \left(\Phi(\mathbf{x}_\mathbf{p}(t)) \mathbf{e}(T)^T P B\right), \quad \hat{\mathbf{W}}(0) = \hat{\mathbf{W}}_0 \tag{24}$$

where positive definite P is the unique solution to the Lyapunov equality

$$0 = A_\mathrm{r}^T P + P A_\mathrm{r} + \underbrace{\begin{bmatrix} 100 & & \\ & 10 & \\ & & 0.1 \end{bmatrix}}_{Q}. \tag{25}$$

Like before the MRAC is tuned for the longitudinal dynamics eq. (21) while neglecting the unmodeled dynamics. The polynomial uncertainties from the dimensionless coefficients do not satisfy the matching condition. Combined with the unmodeled dynamics, the ultimate stability properties of the MRAC cannot be derived using Lyapunov. In the proceeding section, it is shown numerically that the MRAC can tolerate both. With the combined nominal/adaptive control law $u(t) = u_{\mathrm{n}}(t) + u_{\mathrm{a}}(t)$ the new closed loop dynamics eq. (20), eq. (21), eq. (22), and eq. (24) can now be written in their compact form

$$\begin{aligned}
\dot{\mathbf{x}}_{\mathbf{1}}(t) &= \mathbf{f}_{\mathbf{1}}(t, \mathbf{x}_{\mathbf{1}}(t), c(t)), & y_1(t) &= \alpha_{\mathrm{r}}(t), & \mathbf{x}_{\mathbf{1}}(0) &= \mathbf{x}_{\mathbf{1}0} \\
\dot{\mathbf{x}}_{\mathbf{2}}(t) &= \mathbf{f}_{\mathbf{2}}(t, \mathbf{x}_{\mathbf{2}}(t), y_1(t), y_3(t), k_1), & \mathbf{y}_{\mathbf{2}}(t) &= \mathbf{x}_{\mathbf{p}}(t), & \mathbf{x}_{\mathbf{2}}(0) &= \mathbf{x}_{\mathbf{2}0} \\
\dot{\mathbf{x}}_{\mathbf{3}}(t) &= \mathbf{f}_{\mathbf{3}}(t, \mathbf{x}_{\mathbf{3}}(t), \mathbf{y}_{\mathbf{2}}(t), k_2, k_3), & y_3(t) &= z_1(t), & \mathbf{x}_{\mathbf{3}}(0) &= \mathbf{x}_{\mathbf{3}0}
\end{aligned} \tag{26}$$

where $\mathbf{x}_{\mathbf{1}}(t) = \mathbf{x}_{\mathbf{r}}(t) \in \mathbb{R}^2$, $\mathbf{x}_{\mathbf{2}}(t) = \left[\, e_\alpha(t),\, \mathbf{x}_{\mathbf{p}}(t),\, \hat{\mathbf{W}}(t) \,\right] \in \mathbb{R}^3$, $\mathbf{x}_{\mathbf{3}}(t) = \mathbf{z}(t) \in \mathbb{R}^2$, and $\mathbf{y}_{\mathbf{2}}(t) \in \mathbb{R}^2$.

4.2 Validation Problem & Main Results

We want to validate our closed-loop model in its compact form eq. (26) by finding the initial state that maximizes the norm of the concave cost function of the tracking error $J = -(\alpha(T) - c(t))^2$ with given command signal $c(t) = 10\frac{\pi}{180}$ and terminal time $T = 10$. If we can show that for every chosen initial state

$$\begin{aligned}
\mathbf{x}_{\mathbf{1}}(0) &\in \left[\, -1 \times 10^{-6},\, 1 \times 10^{-6} \,\right]^3 \frac{\pi}{180} \triangleq X_{10} \\
\mathbf{x}_{\mathbf{2}}(0) &\in \left[\, -5,\, 5 \,\right]^3 \frac{\pi}{180} \times \left[\, -1 \times 10^{-6},\, 1 \times 10^{-6} \,\right] \triangleq X_{20} \\
\mathbf{x}_{\mathbf{3}}(0) &\in \left[\, -0.01,\, 0.01 \,\right]^2 \triangleq X_{30}
\end{aligned}$$

all trajectories remain bounded in the box

$$\begin{aligned}
\mathbf{x}_{\mathbf{1}}(t) &\in \left[\, -30,\, 30 \,\right]^2 \frac{\pi}{180} \times \left[\, -60,\, 60 \,\right] \frac{\pi}{180} \triangleq X_1 \\
\mathbf{x}_{\mathbf{2}}(t) &\in \left[\, -30,\, 30 \,\right]^2 \frac{\pi}{180} \times \left[\, -60,\, 60 \,\right] \frac{\pi}{180} \times \left[\, -5,\, 5 \,\right] \triangleq X_2 \\
\mathbf{x}_{\mathbf{3}}(t) &\in \left[\, -3,\, 3 \,\right]^2 \triangleq X_3
\end{aligned}$$

until they reach the final state belonging to the set $\alpha(T) \in \{J \leq 3 \times 10^{-3}\} \triangleq X_{1T}$, then the control law is validated. This general description can be expressed by its polynomial dynamical optimization problem

$$\begin{aligned} J = \inf_{x} \quad & -(\alpha(T) - c(t))^2 \\ \text{s.t.} \quad & \dot{\mathbf{x}}_1(t) = \mathbf{f_1}(t, \mathbf{x_1}(t), c(t)) \\ & \dot{\mathbf{x}}_2(t) = \mathbf{f_2}(t, \mathbf{x_2}(t), y_1(t), y_3(t), k_1) \\ & \dot{\mathbf{x}}_3(t) = \mathbf{f_3}(t, \mathbf{x_3}(t), \mathbf{y_2}(t), k_2, k_3) \\ & \mathbf{x_1}(0) \in X_{10}, \quad \mathbf{x_1}(t) \in X_1, \quad \mathbf{x_1}(T) \in X_{1T}, \\ & \mathbf{x_2}(0) \in X_{20}, \quad \mathbf{x_2}(t) \in X_2, \quad \mathbf{x_2}(T) \in X_2, \\ & \mathbf{x_3}(0) \in X_{30}, \quad \mathbf{x_3}(t) \in X_3, \quad \mathbf{x_3}(T) \in X_3, \\ & t \in [\,0,\, T\,], \quad u \in [\,-k_{max}\ k_{max}\,]. \end{aligned} \tag{27}$$

Its approximation in the space of infinite dimensional measures using parsimony can be written as

$$\begin{aligned} J_\infty = \inf \quad & -\int (\alpha(T) - c(t))^2 d\mu_T \\ \text{s.t.} \quad & \frac{\partial \mu}{\partial t} + \text{div}\mathbf{f_1}\mu(t, \mathbf{x_1}) + \mu_T = \mu_0 \\ & \frac{\partial \nu}{\partial t} + \text{div}\mathbf{f_2}\nu(t, \mathbf{x_2}, y_1, y_3, k_1) + \nu_T = \nu_0 \\ & \frac{\partial \xi}{\partial t} + \text{div}\mathbf{f_3}\xi(t, \mathbf{x_3}, \mathbf{y_2}, k_2, k_3) + \xi_T = \xi_0 \\ & \pi_{t,y_1,\#}\mu = \pi_{t,y_1,\#}\nu \\ & \pi_{t,\mathbf{y_2},y_3,\#}\mu = \pi_{t,\mathbf{y_2},y_3,\#}\xi \\ & \int \mu_0 = 1, \quad \int \nu_0 = 1, \quad \int \xi_0 = 1 \end{aligned} \tag{28}$$

Like the results in [23], main advantage of this parsimony approach

The upper bounds for the F-16 polynomial model, coupled flexible dynamics, and combined LQR + MRAC control law can all be found in Tables 8 and 9. The upper bounds obtained using Monte-Carlo can be found in Table 10. The figures for the worst case Monte-Carlo can be found in Figures 10 to 15. The procedure for finding the maximum upper bound is the same as in section 3.

The increased damping inherent from the polynomial model allows for more uncertainty in the unmodeled dynamics. The only case where where the LQR + MRAC cannot tolerate the unmodeled dynamics is when $k_1 = 200,\ k_3 = -200$.

Table 8: Gloptipoly 3 + MOSEK LQR Upper Bounds for Section 4 - Unknown k_1 ($k_2 = -0.1$ $k_3 = 0.1$)

	$k_{\max} = 0.1$		$k_{\max} = 1$		$k_{\max} = 200$	
Rel Ord	**Upper Bnd J**	**CPU [s]**	**Upper Bnd J**	**CPU [s]**	**Upper Bnd J**	**CPU [s]**
1	1.78	1.25×10^1	1.78	9.56	1.78	9.32
2	1.72×10^{-4}	5.22×10^2	1.60×10^{-4}	5.52×10^2	9.78×10^{-4}	6.92×10^2
3	1.00×10^{-5}	1.74×10^4	1.03×10^{-5}	1.80×10^4	1.06×10^{-5}	1.81×10^4

Table 9: Gloptipoly 3 + MOSEK LQR + MRAC Upper Bounds for Section 4 - Uncertain $k_1,\ k_3$ ($k_2 = -0.1$)

	$k_{\max} = 0.1$		$k_{\max} = 1$		$k_{\max} = 200$	
Rel Ord	**Upper Bnd J**	**CPU [s]**	**Upper Bnd J**	**CPU [s]**	**Upper Bnd J**	**CPU [s]**
1	1.42	1.13×10^1	1.42	8.77	9.07×10^{-1}	1.17×10^1
2	9.23×10^{-4}	7.98×10^2	9.29×10^{-4}	7.45×10^2	9.07×10^{-1}	4.68×10^2
3	1.51×10^{-5}	1.82×10^4	1.52×10^{-5}	1.59×10^4	6.42×10^{-1}	1.73×10^4

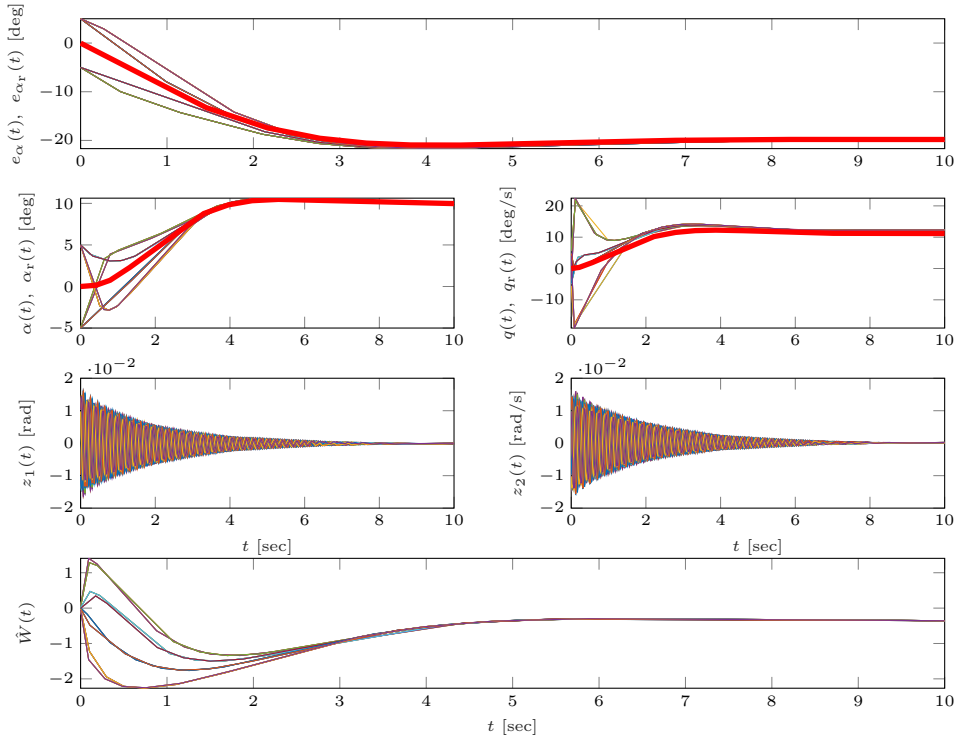

Figure 10: F-16 Polynomial Monte-Carlo Worst Case for Section 4 - Uncertain k_1 - ($k_1 = -1$, $k_2 = -0.1$, $k_3 = 0.1$)

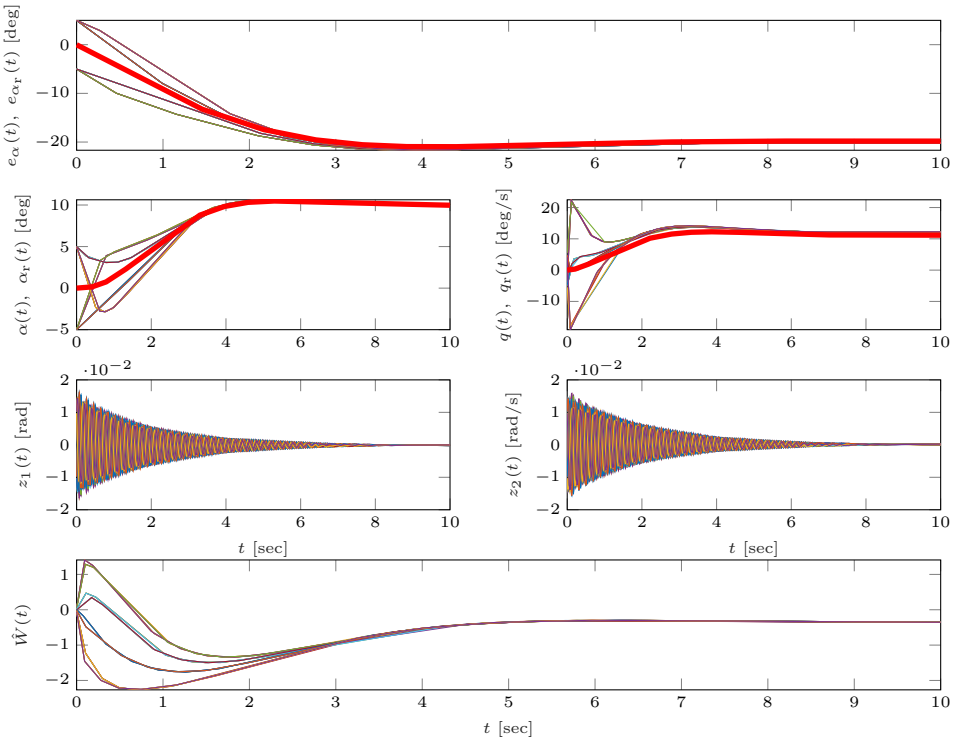

Figure 11: F-16 Polynomial Monte-Carlo Worst Case for Section 4 - Uncertain k_1 - ($k_1 = -10$, $k_2 = -0.1$, $k_3 = 0.1$)

Table 10: F-16 Polynomial Monte-Carlo Upper Bounds for Section 4

	Uncertain k_1		**Uncertain $k_1,\ k_3$**	
$k_{\max}$	**Upper Bnd J**	**CPU [s]**	**Upper Bnd J**	**CPU [s]**
0.1	2.61×10^{-8}	4.82×10^{1}	2.61×10^{-8}	1.82×10^{3}
1	2.62×10^{-8}	4.54×10^{1}	2.70×10^{-8}	2.35×10^{3}
200	2.86×10^{-8}	4.54×10^{1}	1.70×10^{-11}	7.23×10^{3}

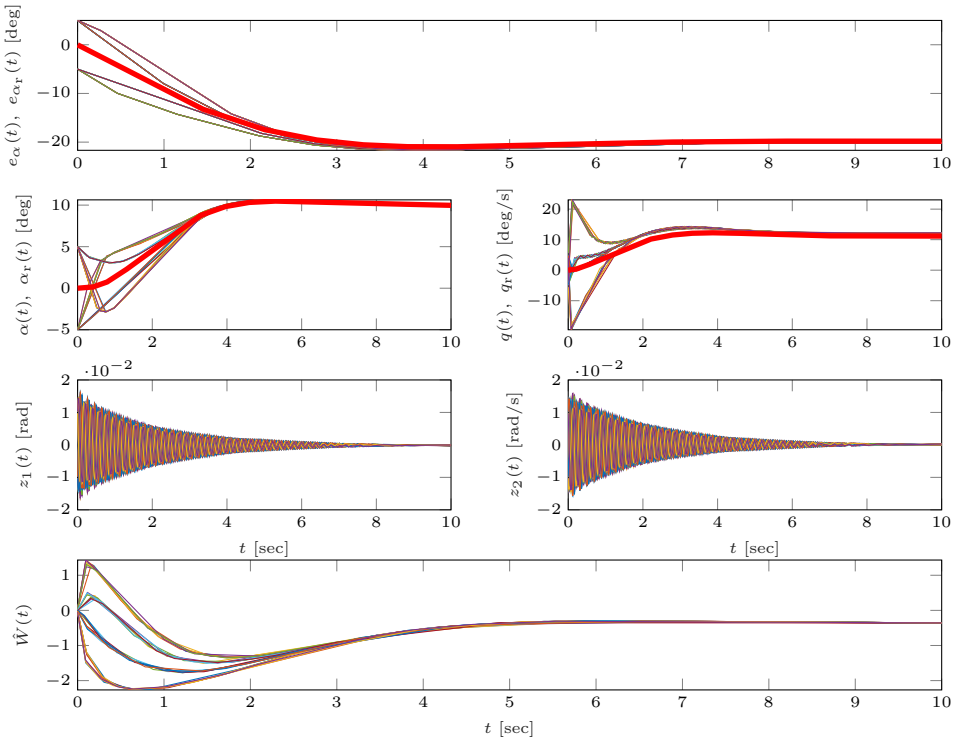

Figure 12: F-16 Polynomial Monte-Carlo Worst Case for Section 4 - Uncertain k_1 - ($k_1 = 200$, $k_2 = -0.1$, $k_3 = 0.1$)

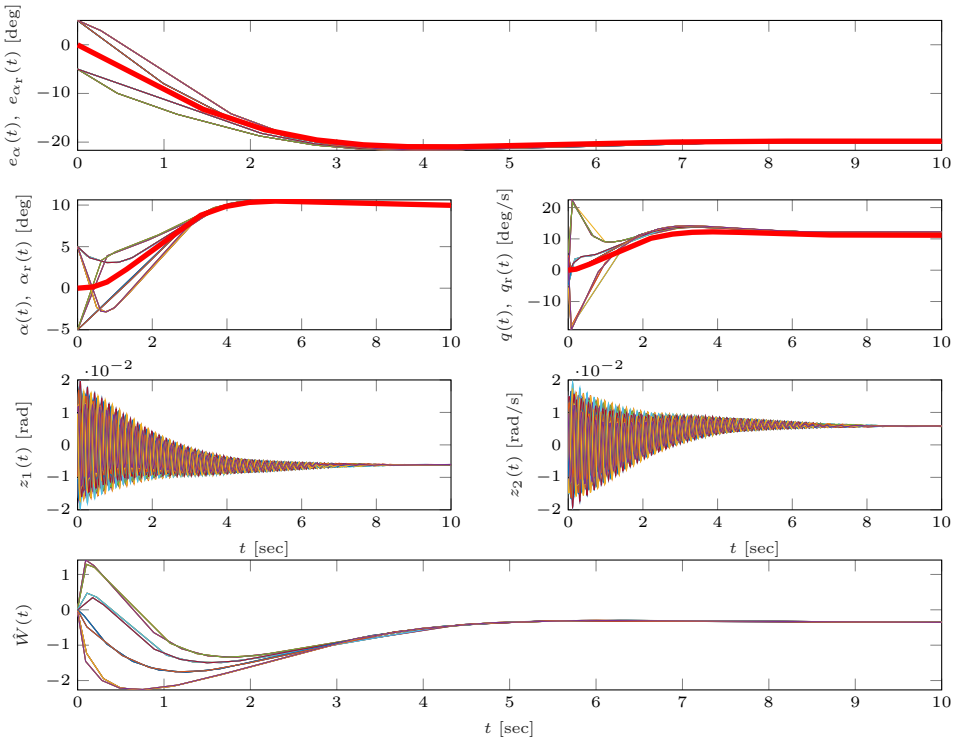

Figure 13: F-16 Polynomial Monte-Carlo Worst Case for Section 4 - Uncertain $k_1,\ k_3$ - ($k_1 = -1$, $k_2 = -0.1$, $k_3 = -1$)

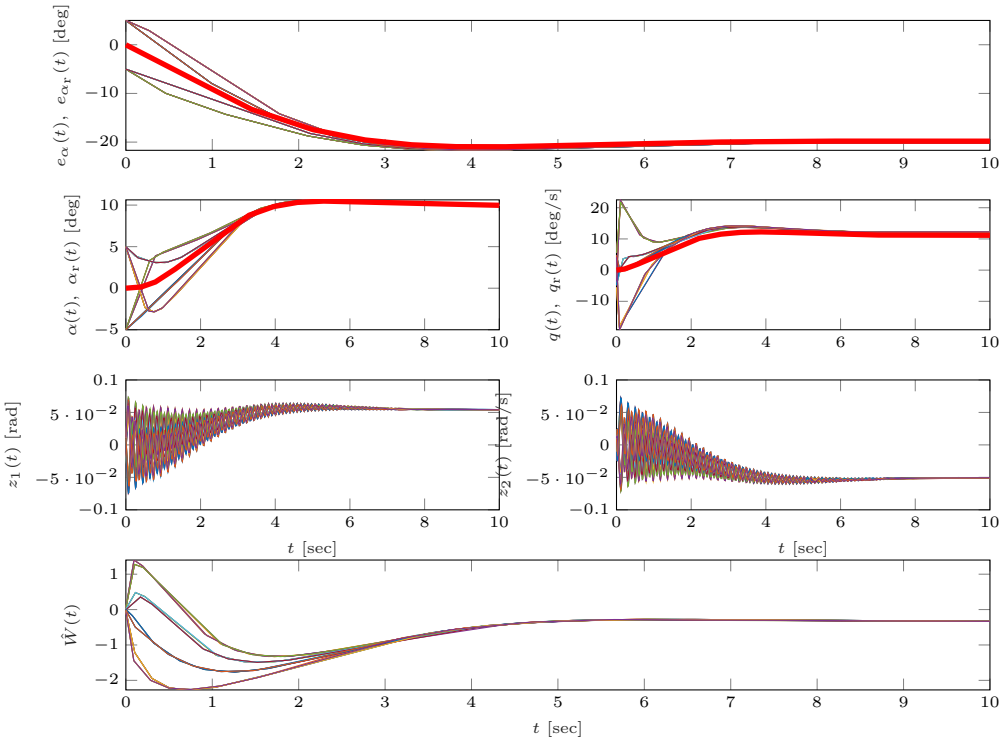

Figure 14: F-16 Polynomial Monte-Carlo Worst Case for Section 4 - Uncertain $k_1,\ k_3$ - ($k_1 = 10$, $k_2 = -0.1,\ k_3 = 10$)

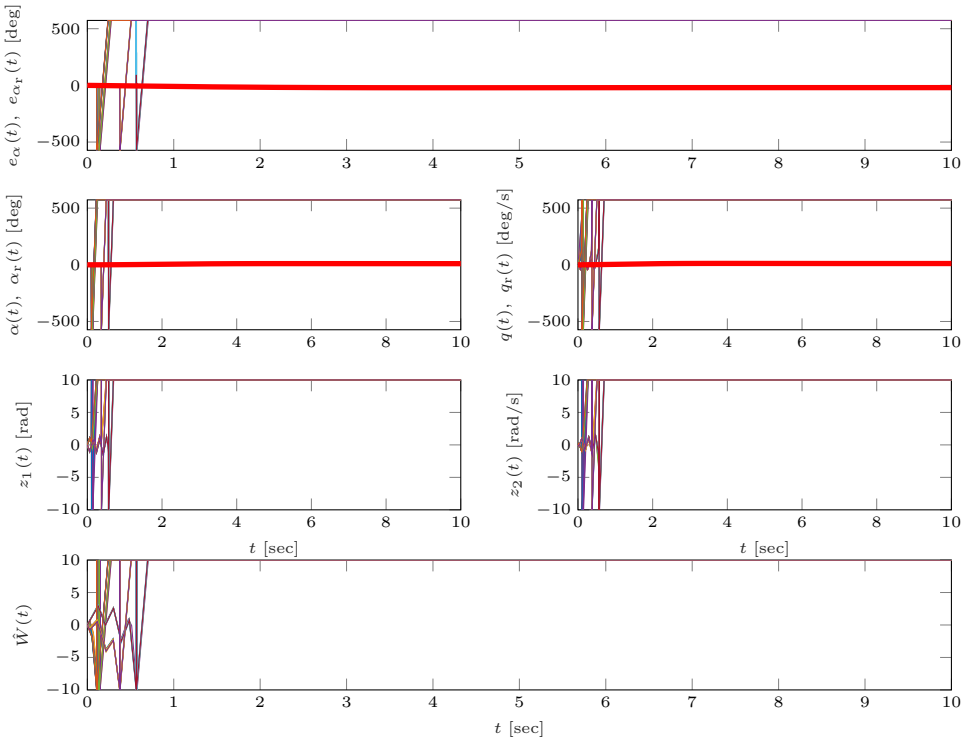

Figure 15: F-16 Polynomial Monte-Carlo Worst Case for Section 4 - Uncertain $k_1,\ k_3$ - ($k_1 = 200$, $k_2 = -0.1,\ k_3 = -200$)

5 Conclusion

We validated both a linear and polynomial F-16 model coupled with uncertain flexible dynamics and MRAC using our VV framework. The state dynamics were approximated and partitioned by exploiting parsimony for ODEs. These results were compared to the upper bounds obtained using traditional Monte-Carlo simulation. This approach allows engineers to address explicitly MRAC interacting with unmodeled dynamics without using costly Monte-Carlo simulations or complex controller modifications. In the future, we hope to use this same framework for validation of a full nonlinear F-16 model complete with MRAC and in-state uncertainties.

References

References

[1] C. Rohrs, L. Valavani, M. Athans, , and G. Stein, "Robustness of continuous-time adaptive control algorithms in the presence of unmodeled dynamics," *IEEE Transactions on Automatic Control*, vol. 30, no. 9, pp. 881–889, 1985.

[2] A. Calise, N. Hovakimyan, and M. Idan, "Adaptive output feedback control of nonlinear systems using neural networks," *Automatica*, vol. 38, no. 8, pp. 1201–1211, 2001.

[3] N. Hovakimyan, F. Nardi, A. Calise, and N. Kim, "Adaptive output feedback control of uncertain nonlinear systems using single-hidden-layer neural networks," *IEEE Transactions on Neural Networks*, vol. 13, no. 6, pp. 1420–1431, 2002.

[4] S. Tong, T. Wang, Y. Li, and H. Zhang, "Adaptive output feedback control of uncertain nonlinear systems using single-hidden-layer neural networks," *IEEE Transactions on Neural Networks*, vol. 13, no. 6, pp. 1420–1431, 2014.

[5] S. Tong, T. Wang, and Y. Li, "Fuzzy adaptive actuator failure compensation control of uncertain stochastic nonlinear systems with unmodeled dynamics," *IEEE Transactions on Fuzzy System*, vol. 22, no. 3, pp. 563–574, 2014.

[6] Y. Li, S. Sui, and S. Tong, "Adaptive fuzzy control design for stochastic nonlinear switched systems with arbitrary switchings and unmodeled

dynamics," *IEEE Transactions on Cybernetics*, vol. 47, no. 2, pp. 403–414, 2016.

[7] M. Matsutani, A. M. Annaswamy, T. E. Gibson, and E. Lavretsky, "Trustable autonomous systems using adaptive control," Proceedings of the IEEE Conference on Decision and Control, (Orlando, FL), December 12–15 2011.

[8] M. Matsutani and A. M. Annaswamy, "Guaranteed delay margins for adaptive control of scalar plants," Proceedings of the IEEE Conference on Decision and Control, (Maui, HI), December 10–13 2012.

[9] M. Matsutani, A. M. Annaswamy, and E. Lavretsky, "Robust adaptive control in the presence of unmodeled dynamics: A counter to Rohrs's counterexample," Proceedings of the AIAA Guidance Navigation and Control Conference, (Boston, MA), August 19–22 2013.

[10] K. Merve Dogan, B. C. Gruenwald, T. Yucelen, and J. A. Muse, "Relaxing the stability limit of adaptive control systems in the presence of unmodelled dynamics," *International Journal of Control*, vol. 91, no. 8, pp. 1774–1784, 2018.

[11] K. Merve Dogan, B. C. Gruenwald, T. Yucelen, and J. A. Muse, "Relaxing the stability limit of adaptive control systems in the presence of unmodelled dynamics," *International Journal of Robust and Nonlinear Control*, vol. 91, no. 8, pp. 1774–1784, 2016.

[12] K. Merve Dogan, T. Yucelen, and J. A. Muse, "Performance guarantees in adaptive control of uncertain systems with unmodeled dynamics," Proceedings of the AIAA Guidance, Navigation, and Control Conference, (Orlando, FL), January 6–10 2020.

[13] K. Merve Dogan and J. A. Yucelen, T Muse, "Adaptive control of dynamical systems with unstructured uncertainty and unmodeled dynamics," Proceedings of the American Control Conference, (Philadelphia, PA), July 10–12 2019.

[14] K. Merve Dogan, T. Yucelen, J. Yildirim, and J. A. Muse, "Experimental results of a model reference adaptive control law on an uncertain system with unmodeled dynamics," Proceedings of the AIAA Guidance, Navigation, and Control Conference, (San Diego, CA), January 7–11 2019.

[15] AIAA Intelligent Systems Technical Committee, "Roadmap for intelligent systems in aerospace," tech. rep., AIAA, 2016.

[16] A. Chakraborty, *Nonlinear Robustness Analysis Tools for Flight Control Law Validation and Verification*. PhD thesis, University of Minnesota, 2012.

[17] A. Chakraborty, P. Seiler, and G. J. Balas, "Susceptibility of F/A-18 flight controllers to the falling-leaf mode: Nonlinear analysis," *AIAA Journal of Guidance, Control, and Dynamics*, vol. 32, no. 1, pp. 73–85, 2011.

[18] D. Henrion, M. Ganet-Schoeller, and S. Bennani, "Measures and LMI for space launcher robust control validation," vol. 7 of *Proceedings of the IFAC Symposium on Robust Control Design*, (Copenhagen, DK), pp. 236–241, 2011.

[19] D. Wagner, D. Henrion, and M. Hromčík, "Measures and LMIs for adaptive control validation," Proceedings of IEEE Conference on Decision and Control, (Nice FR), December 11–13 2019.

[20] D. Henrion, J. B. Lasserre, and J. Löfberg, "Gloptipoly 3: moments, optimization and semidefinite programming," *Optimization Methods and Software*, vol. 24, no. 4–5, pp. 761–779, 2009.

[21] M. ApS, "The MOSEK optimization toolbox for Matlab manual," 2019. www.mosek.com/, (accessed September 15, 2020).

[22] J. Sturm, "Using SeDuMi 1.02, a MATLAB toolbox for optimization over symmetric cones," *Optimization Methods and Software*, vol. 11–12, pp. 625–653, 1999.

[23] D. Wagner, D. Henrion, and M. Hromčík, "Measures and LMIs for lateral F-16 mrac validation," Proceedings of the American Control Conference, (Denver, CO), July 1–3 2020.

[24] J. B. Lasserre, *Moments, positive polynomials and their applications*. London: Imperial College Press, 2009.

[25] M. Tacchi, C. Cardozo, D. Henrion, and J. B. Lasserre, "Approximating regions of attraction of a sparse polynomial differential system," IFAC World Congress, (Berlin, DE), July 12–17 2020.

[26] J. Noel, L. Renson, G. Kerschen, B. Peeters, S. Manzato, and J. Debille, "Nonlinear dynamic analysis of an F-16 aircraft using GVT data," Proceedings of the International Forum on Aeroelasticity and Structural Dynamics, (Bristol, UK), 2014.

[27] M. L. Fravolini, E. Arabi, and T. Yucelen, "A model reference adaptive control approach for uncertain dynamical systems with strict component-wise performance guarantees," Proceedings of AIAA Guidance, Navigation, and Control Conference, (Kissimmee, FL), January 8–12, 2018.

[28] K. S. Narendra and A. M. Annaswamy, "A new adaptive law for robust adaptation without persistent excitation," *IEEE Transactions on Automatic Control*, vol. 32, no. 2, pp. 134–145, 1987.

[29] B. L. Stevens, F. L. Lewis, and E. N. Johnson, *Aircraft control and simulation: Dynamics, controls design, and autonomous systems: Third edition*. NY: Wiley, 3rd ed. ed., 2015.

A Validation Script

```
% inputs
r = input('Relaxation order r = '); T = input('Terminal time T = ');

ki  = 0.1; % uncertain parameter u upper bound

TScaled = 1; % normalized time

xmax = 1 * ones(2,1); x0max = 0.1 * ones(2,1);
zmax = 1 * ones(3,1); z0max = 0.1 * ones(3,1);

Dx  = diag(1./xmax); Dxinv = inv(Dx);
Dz  = diag(1./zmax); Dzinv = inv(Dz);

xmax = Dx * xmax; x0max = Dx * x0max; % normalize all states
zmax = Dz * zmax; z0max = Dz * z0max;

mpol('x1', 2); mpol('z1', 3); mpol('k1', 1); % dynamics

mpol('x0', 2); mpol('z0', 3); mpol('k0', 1); % initial
mpol('xT', 2); mpol('zT', 3); mpol('kT', 1); % terminal

mpol('t1', 1); % measures depend on time
```

```
m1 = meas([x1; z1; k1; t1]); % occupation measures

m0 = meas([x0; z0; k0]); mT = meas([xT; zT; kT]); %initial/terminal measures

% dynamics
x = Dxinv * x1; z = Dzinv * z1; u = k1; t = t1;

A = [0 -1+u 0 0 0; 1+u -5 0 0 0; 0 0.1 -10 0.1 0; 0 0 0.1 -1 -0.1; 0 0 0 1 -1];

f1 = T * blkdiag(Dx, Dz) * A * [x; z];

d = 2*r; % order of relaxation

p1 = genpow(8,d); p1 = p1(:,2:end); % powers

g1 = mmon([x1; z1; k1; t1],d); % bkild test functions

y10 = ones(size(p1,1),1)*[x0; z0; k0; 0]';  % unknown moments of initial measure
y10 = mom(prod((y10.^p1)')');

y1T = ones(size(p1,1),1)*[xT; zT; kT; TScaled]'; % unknown moments of terminal measure
y1T = mom(prod((y1T.^p1)')');

cost = mom(xT'*xT); % input LMI moment problem

A1y = mom(diff(g1,[x1;z1])*f1) + mom(diff(g1,t1)); % linear regime

% bounds on states
X0 = [x0.^2 <= x0max.^2; z0.^2 <= z0max.^2];
XT = [xT.^2 <= xmax.^2; zT.^2 <= zmax.^2];
B  = [x1.^2 <= xmax.^2; z1.^2 <= zmax.^2];

% bounds on time variables [normalized]
Tlim = [t1 >= 0, t1 <= TScaled];

% bounds on uncertain parameter
K0 = k0.^2 <= ki.^2; KT = kT.^2 <= ki.^2; K  = k1.^2 <= ki.^2;

tic % timer
P = msdp(max(cost),...
    mass(m0) == 1,...
    A1y - y1T + y10 ==  0,...
    X0, XT, B, K, K0, KT, Tlim);

% solve LMI moment problem
[status,obj] = msol(P);
```